2016-06-01

Quantifying Computer Vision Model Quality Using Various Processing Techniques

Samantha Anna Ruggles
Brigham Young University

Quantifying Computer Vision Model Quality Using Various Processing Techniques

Samantha Anna Ruggles

A thesis submitted to the faculty of
Brigham Young University
in partial fulfillment of the requirements for the degree of

Master of Science

Kevin W. Franke, Chair
John Hedengren
Gus P. Williams

Department of Civil and Environmental Engineering

Brigham Young University

June 2016

ABSTRACT

Quantifying Computer Vision Model Quality Using
Various Processing Techniques

Samantha Anna Ruggles
Department of Civil and Environmental Engineering, BYU
Master of Science

Recently, the use of unmanned aerial vehicles (UAVs) has increased in popularity across several industries. Most notable, however, is the impact that this technology has had in research at academic institutions worldwide. As the technology for UAVs has improved, with that comes easier to operate, more accessible equipment.

UAVs have been used in various types of applications and are quickly becoming a preferred method of studying and analyzing a site. Currently, the most common use of a UAV is to monitor a location of interest to a researcher that is difficult to gain access to otherwise. The UAV can be altered to meet the needs of any given project and this versatility has contributed to their popularity. Often, they are equipped with a type of remote sensor that can gather information in the form of images, sounds, heat, or light.

Once data has been gathered from a site, it is processed and modified, allowing it to be studied and analyzed. A process known as Structure from Motion (SfM) creates a 3D digital terrain model from camera images captured through the use of a UAV. SfM is a common method of processing the vast amount of images that are taken at a site and the 3D model that it creates is a helpful resource for analysis.

These digital models, while useful, are oftentimes created at an unknown accuracy. This research presents a comparative study of the accuracies obtained when different parameters are applied during the SfM process. The results present a comparison of the time required to process a particular model and the accuracy that the model had. Depending on the application and type of project, a desired level of accuracy can be obtained in the presented amount of time. This particular study used a landslide as the site of interest and captured the imagery using a helicopter UAV.

Keywords: UAVs, remote sensing, structure from motion, landslide monitoring, computer vision

ACKNOWLEDGEMENTS

There are many people that made this research and thesis possible through their support and I would like to take this opportunity to thank them. Firstly, I would like to express gratitude to my advisor, Dr. Franke. He gave me an opportunity and experience that I will forever be grateful for. I appreciate his willingness to teach and guide me through this process and for his insight and advice throughout my schooling.

Thank you also to all of my fellow students who assisted me in my research and provided support and encouragement; Derek Wolfe, Abe Martin, Brandon Reimschiissel, and Chris Bender. They were always willing to help with and solve any problems that arose. A big thank you also to my graduate committee, Dr. John Hedengren and Dr. Gus Williams, for reviewing my work and providing valuable feedback.

Funding for this research was made possible by the generous efforts of the Center for Unmanned Aircraft Systems and its members. This research was part of the BYU project 13-03 and I am grateful for the opportunity to have worked with such generous, intelligent people.

Lastly, I would like to thank my biggest support system, my family. They have always supported and encouraged me throughout this project and my life. I cannot thank them enough for their encouragement, love and willingness to help me in any way possible. Thank you Mom, Dad, David, Jon, Megan, and my wonderful fiancé, Keith.

TABLE OF CONTENTS

TITLE PAGE ..... **i**
ABSTRACT ..... **ii**
ACKNOWLEDGEMENTS ..... **iii**
TABLE OF CONTENTS ..... **iv**
LIST OF TABLES ..... **vi**
LIST OF FIGURES ..... **vii**

1 Introduction **1**
1.1 Background 2
1.1.1 Landslide Monitoring 5
1.1.2 Environmental Applications 11
1.1.3 Infrastructure Monitoring 13
1.1.4 Other Applications 16
1.1.5 Custom Built UAVs 19
1.1.6 Current Study 20
2 Methodology **23**
2.1 Site History 24
2.2 Hardware 25
2.2.1 UAV 25
2.2.2 Camera 27
2.2.3 Computer 28
2.3 Software 29
2.3.1 Agisoft Photoscan 29
2.3.2 Cloud Compare 30
2.3.3 Xn Convert 30
2.4 Different Parameters 30

2.4.1 GCPs 31
2.4.2 Camera GPS 34
2.4.3 Processing Quality 35
2.4.4 Masking 36
2.5 Workflow 38
2.5.1 Collecting the Data 38
2.5.2 Establishing Ground Truth 39
2.5.3 Pre-processing 41
2.5.4 Processing 43
2.5.5 Comparing the Data Sets 45
3 Results 48
3.1 Accuracy 48
3.1.1 Georeferencing 49
3.1.2 Processing Quality 51
3.1.3 Masking 54
3.2 Resolution 54
3.3 Chapter Summary 55
4 Conclusion/Recommendations 57
4.1 Conclusions 57
4.2 Recommendations for Future Research 59
References 60
Appendix A. Model Time Contribution Breakdown 63
Appendix B. Model Accuracies 72

LIST OF TABLES

Table 2-1: Study Matrix Naming Scheme 31

Table 3-1: Accuracy of Model Comparisons 48

Table 3-2: Time for Model Creation 49

Table 3-3: Model Resolution 54

Table 3-4: Quantitative Results Summary 56

LIST OF FIGURES

Figure 1-1: Various Types of Remote Sensors 3

Figure 1-2: Multirotor UAVs 4

Figure 1-3: Quadrotor UAV 4

Figure 1-4: Structure from Motion Illustration 7

Figure 1-5: Typical LiDAR Setup 8

Figure 2-1: North Salt Lake Landslide 25

Figure 2-2: Align 800 Helicopter UAV 26

Figure 2-3: Align G3 Gimbal 27

Figure 2-4: Nikon D7100 DSLR Camera 28

Table 2-1: Study Matrix Naming Scheme 31

Figure 2-5: Aerial Photos of GCPs 32

Figure 2-6: GCP Marker Used for This Study 33

Figure 2-7: Topcon GR-3 Survey Equipment 33

Figure 2-8: Geotagger Pro 2 Solmeta 34

Figure 2-9: Masking Process 37

Figure 2-10: FARO Focus 330 LiDAR Scanner 40

Figure 2-11: Terrestrial LiDAR Point Cloud Model 41

Figure 2-12: Agisoft Point Clouds – (a) Sparse Cloud (b) Dense Cloud 44

Figure 2-13: Segmented Comparisons Along Face of Landslide 46

Figure 2-14: Model Comparisons – (a) TLS Model (b) SfM Model 47

Figure 3-1: Close Up Detail of (a) Medium and (b) High SfM Point Clouds 53

1 INTRODUCTION

Unmanned aerial vehicles (UAVs) have recently been moving to the forefront of research and development throughout several industries and academic institutions. As the technology required for UAVs has become more advanced, it has played a greater role in scientific research, data collection, and reconnaissance operations. The appeal of these aircraft is their automation, agility, and versatility.

UAVs can be controlled remotely through the use of a computer program or a human pilot. Autonomy can vary between each vehicle and the more autonomous a drone is, the less it will have to rely on manual piloting and controls.

Another reason drones are increasing in popularity is their ability to access areas and spaces that otherwise would be inaccessible to humans due to dangerous terrain and conditions. UAVs are able to gain information from sites that would otherwise remain unknown to researchers (Immerzeel et al., 2014). Their small size and easy maneuverability allows them to do this without endangering lives. A hazardous site, such as that found after a landslide or earthquake, can quickly be flown over with a UAV to assess the damage and construct an accurate reconnaissance report (Adams and Friedland, 2011). In some cases, hazards can be prevented through early detection done through the monitoring of a site with UAV-mounted sensors.

UAVs are becoming an increasingly widespread way to collect field research because of their versatility. Drones are available in hundreds of configurations and can be custom made to suit any research or commercial purpose. They are equipped with a remote sensor for capturing data, which is commonly a camera (Lucieer et al., 2013). Other types of remote sensors, that collect data other than visual images, can be installed to allow for various applications and projects. The vast availability of UAVs and different sensors allows for them to be used for various applications, making them an easy option for aerial data collection.

Any area of interest that is difficult or dangerous to obtain valuable research data from can more easily be retrieved through the use of drones. They allow for easy, remote control while data is gathered more quickly and efficiently than through manual practices. Different applications will be discussed more in-depth in the next section of this chapter. These previous case studies showcase the versatile nature and characteristics that make UAVs the preferred method to remotely collect data.

For the study presented in this report, a UAV and remote sensor were used to assess the accuracy that can be obtained in a 3D digital terrain model of a local landslide. Based on different input parameters needed to create the models, the accuracies were quantified and compared against one another to determine which one produced the most accurate model in the shortest amount of time.

1.1 Background

Remote sensing is the process of obtaining information about an area of interest through the use of sensors that can relay the information without having to make physical contact with the site. There are various forms of sensors that collect visual, acoustic, thermal, and

hyperspectral data from a study site. Many different types of sensors are used to obtain this information, including cameras, LiDAR, radar, and satellites, as shown in Figure 1-1.

Figure 1-1: Various Types of Remote Sensors

For many of the studies described in the following sections, a camera was used to collect images (Room and Ahmad, 2013). A camera is a common method for remote sensing due to its versatility and ability to capture a large amount of valuable data. With the wide array of commercial cameras available, there is an option available for every type of application and project. Images can be captured at a specified resolution and quality, depending on the desired level of detail. The process of photogrammetric remote sensing has been used for several decades and is a convenient, low-cost way to monitor a site. A recent development in the field of remote sensing is the use of UAVs to transport sensors.

Several different sizes of UAVs are available and can be selected based on many different factors. Larger platforms, including the multirotor in Figure 1-2 and the helicopter can carry a heavier payload and bigger sensors. Smaller aircraft, such as the quadrotor in Figure 1-3, while

not able to transport as much equipment as the larger ones, can be ideal for smaller projects or maneuvering around tight areas. They also require less experience and training to operate than the larger UAVs. Researchers can determine which platforms they want to use based on the size and scope of a project and what kind of data they want to remotely obtain.

Figure 1-2: Multirotor UAVs

Figure 1-3: Quadrotor UAV

Many of the current UAV related studies involve testing a single type of platform and analyzing its effectiveness given a specific task (Matese et al., 2015; Strecha et al., 2008). These

tasks have involved monitoring and recording change that occurs in landslides, unpaved roads, and coastal environments as well as quantifying the impact of erosion (Merz and Kendoul, 2011; Siachalou et al., 2015). High resolution imagery captured aerially has provided researchers with valuable information for several types of sites. Several of these case studies have examined an area of geotechnical or environmental significance. In studying these areas with drones, researchers have developed several workflows and processes to analyze the data that is collected. Platforms, sensors, computer processors, and software have all been modified to meet the specific needs of a project.

1.1.1 Landslide Monitoring

Lucieer et al (2014) presented a cost-effective, flexible, and accurate method used to monitor an active landslide in southeast Tasmania using a UAV mounted with a commercial optical sensor. To achieve this, several 3D digital reconstructions of the landslide were made over a period of several days, and a change detection analysis was performed to map displacements. The platform used for this study was a small multirotor UAV measuring 80 cm in diameter and weighing in at 3 kilograms, equipped with a Canon 550D Digital Single Lens Reflex (DSLR) camera mounted onto a motion-compensated gimbal to capture the photos. A gimbal is a support mechanism for the camera that only allows rotation about a single axis. It acts as a stabilizer against the motions and vibrations that occur during a flight, allowing for clear images to be taken.

Ground control points (GCPs) were established during this study in order to improve the accuracy of the 3D models. The GCP markers, created with aluminum disks placed around the site and recorded using GPS receivers, were used to georeference the models in a real world coordinate system.

Thirty-nine aluminum disks were distributed around the site and were manually identified in the images so they could be georeferenced and make the models more precise. In doing so, many researchers have found that the accuracy of their models is improved. Another achievement of this study was the minimizing of the alignment error to +/- 0.07 meters on average.

Structure from motion (SfM) technologies have recently emerged as the leading way to recreate 3D digital terrain models using digital imagery (Mancini et al., 2013; Piermattei et al., 2015). The process is inexpensive, quick, and user friendly. After the images at a given site have been collected, the SfM process is implemented to build the 3D digital models. To give a brief overview, structure from motion is a method of creating three-dimensional models from two dimensional images (Koska and Kremen, 2013). This is done through an algorithm that varies depending on the software performing the image reconstruction. SfM is a fairly new technology that, coupled with photogrammetry gathered with UAVs, is becoming the favored method for analyzing data over Light Detection and Ranging (LiDAR) (Bellian et al., 2005). SfM relies on overlapping, offset photos taken of the same object or site using a mobile sensor as the name implies. Figure 1-4 shows a brief, easy to understand illustration of how the SfM process works. Using the camera position, angle, and orientation of the photo, a textured 3D model is generated by aligning similar features that appear within each photo. Employing SfM techniques yields results that are comparable and in some cases, exceed those gathered through terrestrial LiDAR (Wallace et al., 2014).

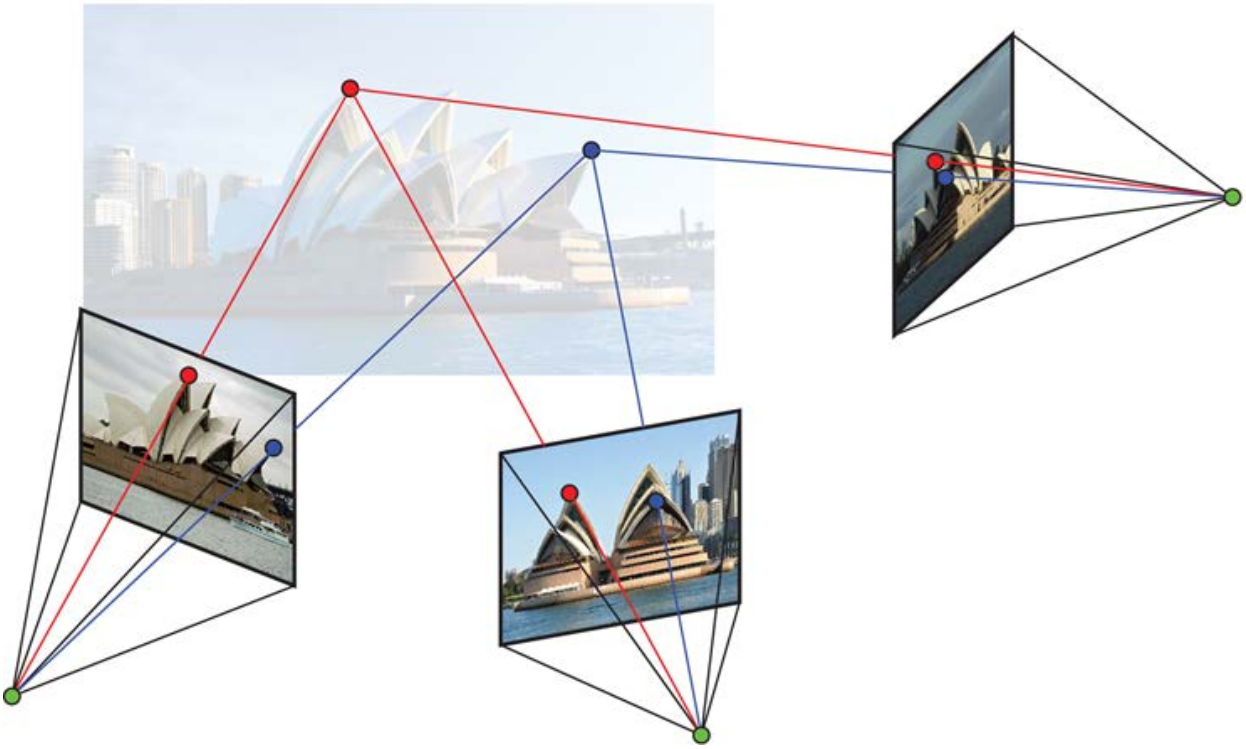

Figure 1-4: Structure from Motion Illustration

LiDAR is the process of detecting objects and distances through the use of lasers. The light from the laser reflects off the surface of a target object and the unit is able to pick up the beam and calculate how far away the object is. There are many different types of LiDAR available that have been used in several different applications. It has been used to gather photogrammetry and create digital surface models (Buckley et al., 2008). Typically, the LiDAR sensor is mounted onto a manned aircraft and flown over a large area (Trier et al., 2012), as presented in Figure 1-5. Gathering data over such a broad region can, however, lead to lower resolution data. Depending on the quality of the unit, LiDAR can produce digital models that are accurate within millimeters of the actual ground truth (Stumpf et al., 2013).

Figure 1-5: Typical LiDAR Setup (Merz and Kendoul, 2011)

In the case study taken from Lucieer (2014), the Agisoft Photoscan SfM software (Agisoft LLC, 2011) was used to import and process the photographs. This software was able to generate the 3D reconstructions needed for the change detection analysis using a point matching algorithm. The program scans each image while identifying and matching up distinct features that occur in similar photos. Once all these features, or points, are matched up, a 3D model can be constructed. The final product is a model comprised of a cloud of thousands of individual points that can vary in density depending on the resolution and quality of the images. It is imperative to these reconstructions that the images have sufficient overlap. For the monitoring of the landslide in Tasmania, 80-90% image overlap was used (Lucieer et al., 2014). These images were captured from multiple positions and angles at an average flying height of 40 meters. This height ensured that each photograph covered an area on the ground of approximately 1700 square meters. In order to make the SfM process as efficient and accurate as possible, the photos

were selected manually and chosen based on the visual quality, viewing angle, and overlap. After the models were generated, they were used to calculate ground movement and assessed for accuracy.

The results of this study in Tasmania proved that UAV imagery coupled with a SfM workflow can produce several detailed, accurate 3D models that can successfully be used to monitor and map displacements that occur on a landslide. It was found that the displacements that occurred on the landslide were irregular and dispersed unevenly across different locations. The SfM algorithm was able to more accurately quantify movements in the vegetation, ground material, and toes of the landslide but was less successful in monitoring displacement in the retreat of the main scarp. In testing the accuracy of the models against the established GCPs, the error calculated was 7.4 centimeters horizontally and 6.2 centimeters vertically. During the study, researchers identified ways in which this accuracy could have been worsened due to sources of uncertainty. One specific source mentioned was the different weather and shadow patterns that can alter the images depending on the time of year and day they were taken. A difference in lighting can impact the displacement calculations. While there appeared to be some inaccuracies within this study, researchers Lucieer et al (2014) indicated that the workflow they presented can be used for flexible and accurate monitoring of landslides.

Other researchers have also discovered the usefulness of UAVs in the monitoring of landslides. In 2008, Niethammer et al (2012) combined a quad rotor helicopter with a digital compact camera to obtain photos of the Super-Sauze landslide located in southern France (Walter et al., 2009). Remaining active since the 1970's, this landslide continues to experience 0.01-0.4 meters of movement per day. Such high displacement rates require constant monitoring of the site to ensure safety of the nearby residents. Presented in their study is a new approach to

monitor the active landslide over a long period of time with the aid of UAVs. It was decided that UAVs be used because they are well suited for the terrain and can obtain a significant amount of data relatively easy. A quad-rotor was chosen because of its stability and it was developed to withstand vibrations through the addition of inertial measurement units. To capture the entire landslide, 1486 pictures were taken in an automatic capture mode every three seconds. Once the photos were gathered, a SfM algorithm was able to stitch them together to create a 3D surface model. This particular algorithm did not require any ground control point information, leaving the model without a definite coordinate system. After the generation of the 3D model, an ortho-mosaic and digital surface model could be rendered. These approaches revealed that a high-resolution digital surface model could be created without the use of GCPs. Oftentimes, study areas can be quite hazardous and manually marking and measuring GCPs can be dangerous. The method used by Niethammer et al (2010) is a fitting approach for monitoring these types of sites because it keeps researchers safe by not requiring that GCPs be obtained through unsafe practices. Even without the models being georeferenced, they still had resolution and accuracy that was acceptable to the researchers with up to 70 points per square meter.

The monitoring of landslides is important for prediction and prevention of further damage as researchers are able to track and observe changes in the topography of the site. Stumpf et al (2013) conducted a study to observe the geological patterns that were occurring on an active landslide to gain a better understanding of its history. Gaining a knowledge of the past dynamics of the slide would help them predict future movement, just as many scientists have done so before. In their study they made use of a UAV that was able to capture aerial imagery. From these images, they were able to identify significant features within the slide that indicated history

of stress. These features, or “fissures”, were marked on a digital terrain model and analyzed based on their size, orientation, length, and density.

1.1.2 Environmental Applications

In a study of a coastal site in Tasmania, Australia, researchers Harwin and Lucieer (2012) assessed the accuracy of georeferenced point clouds as they were compared to a Total Station survey of the same area. Using UAV imagery, digital terrain models of the site were created with 12 GCPs included. In quantifying their geometric accuracy, it was found that georeferenced point clouds can be accurate to 25-40 mm. The findings concluded that sub-decimeter change in terrain can be monitored. The images they captured at the site were such high resolution that many small details were able to be identified.

Another environmental application is a soil erosion monitoring project that took place in Morocco (d’Oleire-Oltmanns, 2012; Mancini et al., 2013). The objective here was to obtain high resolution monitoring data of the study area. Using a fixed wing aircraft equipped with a Panasonic digital camera, a gully system and badland region were mapped in order to monitor soil erosion. The site in Morocco was chosen because of its significance to the agricultural industry of the region. This importance makes the area highly desirable for land development but also very fragile and vulnerable which is why it needs constant monitoring to predict and prevent erosion. For this study, GCPs were established around the surface of the gully that were marked with red cardboard squares. This type of marking ensured that they were visible in the photos. Data was successfully acquired at multiple scales and two separate workflows were applied depending on the flying height of the UAV. From these two workflows accuracy values between 0.009-0.3 meters were obtained. Digital Terrain Models (DTMs) and orthophotos were created from the data and from these, soil erosion was able to be monitored and analyzed at a level that

rivals that obtained through field work. These results conclude, once again, that UAVs with remote sensors can be applied to most types of environmental mapping.

Other sites of geotechnical significance have been monitored by UAVs including glaciers, geothermal fields, and open pit mines. (Nishar et al., 2016; Immerzeel et al., 2014; Piermattei et al., 2015; Shahbazi et al., 2015; Arbues et al., 2012; Fernandez et al., 2004) In a recent study of a small glacier in the Italian Alps, terrestrial photogrammetry and SfM was used to estimate mass balance (Piermattei et al., 2015). Typically, information about the surface of glaciers is obtained through LiDAR technologies. However, using structure from motion technology, a low-cost method was developed to achieve results that were comparable to LiDAR. The volume changes and mass balance estimates computed with the 3D models were almost identical to those obtained with the terrestrial laser scans.

During a similar study of a Himalayan glacier, high-resolution monitoring of glacier dynamics was performed with UAVs (Immerzeel et al., 2014). This study was significant because, up to this point, Himalayan glaciers have remained unstudied because of their remote location and treacherous terrain. These glaciers have such an impact on the livelihood of the local people, both as a source of water and hydropower, obtaining as much information about them and their changes is crucial to the Himalayan environment. The existing methods for monitoring these locations consists of infrequent field monitoring from distant locations or space-borne remote sensing which only provides rough images and sparse data. Knowing this, researchers Immerzeel et al. (2014) deployed a UAV with a remote sensor in an attempt to complete the existing knowledge of these glaciers. The UAV chosen for this field work was a fixed wing aircraft with a wingspan of 80 cm that was equipped with a GPS receiver, altimeter, wind meter, and digital camera. It followed a specified flight path and captured images while

maintaining flight speeds of 36 km/h for 30 minute increments. Nineteen GCPs were established in May and October of 2013. For the processing of the images, a SfM workflow was utilized in Agisoft Photoscan to create digital elevation models and ortho-photo mosaics of the glacier. This study, being the first of its kind, proved to be highly successful at quantifying the volume change in the glacier over a period of five months. The use of UAVs shows high potential in the study and exploration of glaciers. Results indicated that the imagery gathered from the UAV was a higher resolution and accuracy than any currently available info. Such information was only available because of the ability of the UAV to access this rarely studied, remote glacier.

1.1.3 Infrastructure Monitoring

In addition to monitoring landslides and other environmental phenomena, UAVs have been utilized in the monitoring and inspection of infrastructure (Ellenberg et al., 2014; Tang and Alaswad, 2012). As infrastructure continues to age, expand, and become more complex, the amount of monitoring required to maintain it is rapidly becoming unsustainable due to limited funds and human resources (Chen et al., 2011). UAVs allow for the automation of infrastructure monitoring which is vital to survival and reliability of these structures, whether it be roads, bridges, pipelines, or canals. When Rathinam et al (2008) monitored local linear structures, they used a UAV and visual feedback to obtain information about a particular site. To improve upon the inspection of structures, they incorporated an imaging sensor that was able to detect the structure, thereby enhancing the accuracy from the GPS. Many long linear structures need to be constantly monitored aerially and using the procedures listed in their study, Rathinam et al (2008) were able to create a way to do that with and without the aid of GPS. This can prove to be particularly useful during times of natural disasters when linear structures are displaced and GPS is unable to locate them. This innovative technique provides a real time solution for detection of

structures. Through this detection, a UAV can then change its flight path to include areas of interest on a structure. The deviation error recorded during this study was around 10 meters over a stretch of 700 meters of a canal. While this particular study did not include research on the processing of this information, there are other studies that have addressed this topic.

In 2009, the condition of the infrastructure in the United States was given a rating of D by the ASCE, along with the classification of 26% of the bridges as structurally deficient (Dobson et al., 2013). With over 600,000 bridges in the country, the inspection, monitoring and repair of these structures can seem quite overwhelming. The visual inspections of these bridges requires a significant amount of time and effort and can be quite risky to the inspector. In most cases, the areas of a bridge that need to be monitored require remote access that are unsafe or require many safety precautions to obtain sufficient data. Another drawback to visual human inspection is the subjective nature of the task. Each individual operator identifies cracks and areas of weakness on a bridge differently depending on their level of experience. All of these limitations lead to discrepancies among different inspectors which can cause delayed, ineffective repairs. To overcome these limitations, UAV photography is starting to become integrated into the monitoring of infrastructure across the country.

UAVs can be used to identify cracks and other anomalies in roads, pipelines, bridges and other structures. In their report for the American Society of Civil Engineers, Ellenberg et al (2014) examined the current and potential use of UAVs for the monitoring and inspection of America's infrastructure. Currently, aerial inspection through the use of a fixed wing aircraft is taking place to remotely sense cracks and potholes in roadways. Chen et al (2011) described the methods of using aerial imagery that was able to successfully detect visible defects on bridge decks. Using this data, stress formations and possible movement within the bridge supersystem

were able to be identified. Within this same study, bridge construction was monitored as a way to determine the surrounding environment, processes, and measurements required to have a seamless construction process. After obtaining the aerial imagery of a bridge site, the photos were imported into ArcGIS where further analysis could be done. While this particular method of bridge monitoring was not meant to replace visual inspection at this point in time, it can be used to enhance the current methods by reducing time and cost.

In their study, Ellenberg et al (2014) deployed a small quadrotor equipped with two cameras and capable of flights lasting 8-12 minutes. The objective of this research effort was to create an unmanned aerial system that was capable of conducting infrastructure inspection similar to that obtained through visual inspection. The UAV imagery was compared against Simultaneous Localization and Mapping (SLAM) technology to determine accuracy. SLAM is the process of mapping an unknown environment while simultaneously keeping track of an object's position within that environment. With a 2-mm accuracy at a 1-m distance, using the SLAM equipment was an inexpensive alternative to LiDAR that allowed for accurate comparisons to the UAV based models. For the post processing of the images, a MATLAB algorithm was developed that had the ability to identify significant deformations and cracks along a structure. The field work on this project involved a pedestrian bridge with precisely placed markers that were easy for the algorithm to detect. The results of the study revealed that the data collected with the UAV would be able to provide accurate results in the detection of defects and damage on infrastructure. These results were even able to produce more quantitative assessments than those acquired through the use of human inspectors, who can often deliver subjective reports that vary depending on the individual. Performing the test on an existing

pedestrian bridge proved the concept of a UAV being able to identify specified irregularities when combined with a MATLAB based algorithm.

1.1.4 Other Applications

In the field of archaeology, 3D models are invaluable to the process of studying and analyzing historical sites. Because the areas of interest typically need to be studied in the field, in remote areas, or places that are a great distance away, providing digital models that can be accessed anywhere is crucial to archaeologists (Eisenbeiss, 2011). Through this study, they were able to achieve 2.5 meter accuracy. The methods that are currently being used include terrestrial laser scanning or fringe protection systems (Kersten and Lindstaedt, 2012). There are several limitations to using either of these types of systems. They are quite bulky to use in a field environment. Often, they require expert knowledge to operate, which only adds to the initial cost by a substantial amount. Recently, however, researchers have been making use of UAVs to obtain imagery because of their flexibility, and convenience (Kelcey and Lucieer, 2013). UAVs can be easily mobilized to any site, allowing for quick set up and take down.

There are several low-cost options for software available for building 3D digital terrain models. In their study, Kersten and Lindstaedt (2012) identified several of these software options and weighed their cost against the accuracy they were able to produce. After obtaining imagery of artifacts from Easter Island, Qatar, and Ethiopia, the photos were processed using four different programs. Each of these programs provided an inexpensive alternative, being either open source or low-cost. At the conclusion of the study, it was determined that these image-based systems were able to create 3D models with enough precision and accuracy to rival that of their more expensive counterparts. In archaeological applications, precision and accuracy are imperative. It was found that while the image-based systems achieved the desired levels of

precision and accuracy, they were also able to accomplish this task in a shorter amount of time than traditional methods. The advantage of using these types of software is that they can create digital models from photographs that can be obtained through UAVs. This requires much less effort than the transporting and setup of the laser based systems.

Recently, the use of UAVs in agricultural applications has proven to be quite effective (Vaaja et al., 2011). Previously, satellite sensors have been employed in the monitoring of significant agricultural areas. However, satellite imagery does not provide enough resolution and it is difficult to obtain data on a schedule that correlates with the availability of the satellite. Researchers Berni et al (2009) were able to overcome these problems through the use of a UAV. A remote sensor was placed on a helicopter UAV and flown over agricultural fields. The sensor was able to obtain thermal and narrowband multispectral imagery. The sensor and platform used was very successful in producing accurate results, allowing the crops to be monitored in a cheap, efficient way. It produced better results than could be obtained through traditional satellite imagery because of its low flight altitude and speed. This allowed for the UAV to gather closer, higher resolution data. From this, Berni et al (2009) were able to make accurate predictions about the biophysical parameters of a crop field, making it the superior method for sensing.

Another application of the UAV is currently increasing in popularity, effectiveness, and usefulness. The concept of employing a UAV for post disaster reconnaissance missions is being implemented around the globe for purposes of safety, mobility, ease, and low cost. Using a UAV for disaster research produces high-resolution images that can be analyzed and used to produce hazard maps, elevation and contour maps, digital surface models, and renderings (Adams and Friedland, 2011). This data can then be used to assess damage, organize rescue efforts, or better understand the effect that natural disasters have on the infrastructure and its surroundings.

Perhaps the most appealing factor in using a UAV for reconnaissance purposes is their ability to observe a site while keeping the operators and researchers safe. Many of the disaster sites that need to be observed are unsafe for humans to acquire data.

In 2005, Hurricane Katrina struck the Gulf Coast, leaving behind a path of destruction (Adams and Friedland, 2011). Buildings, roads, bridges, and utility lines were wiped out, making it very difficult to collect field data. Researchers wanted a way to inspect the response of infrastructure to this disaster yet there was no safe, efficient way of doing that due to the lack of sufficient accommodations and transportation routes. To overcome these limitations, Pratt et al (2006) used a helicopter UAV and a digital camera to capture aerial imagery of several commercial buildings that had suffered damage from the hurricane. This UAV allowed for post-disaster data collection that otherwise would be unobtainable through the use of ground footage only. For this particular study, limitations arose because of the difficult nature of the environment. Limited landing and takeoff space required adjustments to be made and created greater distances to fly to areas of interest. A GPS-based flight hold feature was installed on the UAV which allowed the UAV to hover over a designated spot, leaving the operator free to adjust camera positions to capture the ideal imagery. In the report, Pratt et al. (2006) identified several ways in which UAVs can be improved upon for better post-disaster assessment. They mention the addition of the ability to return to the last known good communications point if the signal between the operator and UAV is broken. Since these suggestions in 2006, several advancements have taken place in the newer UAV systems. While the environments surrounding a post-disaster site can prove to be challenging, UAVs have been the preferred method of data collection because of their ability to keep researchers and operators safe while being versatile enough to adapt to unique situations.

Recent earthquakes have also required the assistance of UAVs for gathering aerial imagery. After the 2010 earthquake in Haiti, a private company deployed a small UAV to assess the damage that was done to an orphanage in the mountains of Port-au-Prince (Quaritsch et al., 2010; Huber, 2011). While relaying images in real time, they were able to determine that the infrastructure was intact, allowing rescue crews to focus their efforts elsewhere instead of spending time on an area that didn't need immediate attention. This real-time imagery collection allows for rapid response of rescue efforts after a natural disaster. Such immediate data acquisition is made possible because of the ability of a UAV to acquire imagery from overhead in these hazardous post-disaster zones.

1.1.5 Custom Built UAVs

As mentioned previously UAVs can be custom built to suit the needs of any project. In a recent study conducted by Cooper et al (2015), a UAV was built for autonomous front-on environmental sensing of a target. The system, which uses a probabilistic model, was created based on low-cost and easily available sensor systems. As the study progressed, it was observed that the accuracy could be increased with higher precision instruments and sensors. Although limitations arose within the system, they were outweighed by the low cost and ease of use. The accuracy that was obtained was adequate enough for the function intended while still maintaining a reasonable price.

A similar situation occurred when Travelletti et al (2012) presented a way to monitor the displacement of an active landslide located in the South French Alps. One of the main requirements of the study was to keep the monitoring methodology at a low cost. In keeping expenses low, it allows for equipment to easily travel to inaccessible areas without the fear of

damaging expensive research supplies. As is the case with any research study, the desired accuracy had to be weighed against the cost. After many trials and experimentation, Travelletti et al (2012) were able to develop a method that allowed for them to track daily movements on the Super-Sauze landslide while still maintaining a low budget. To achieve this, they used open source quad-rotor systems and an inexpensive, compact sensor. The average 3D error measured in this study was 0.14 meters with a standard deviation of 0.56 meters.

Every aspect of the UAV equipment is carefully chosen to accomplish a given research task. In his thesis, Li-Chee-Ming (2012) describes in great detail the development of a mobile stereo mapping system (MSMS) to be used onboard a UAV. The purpose of the MSMS is to perform efficient, geoferenced mapping in areas that are unsafe for human access. It was designed to be lightweight, portable, and easily transferrable across different platforms. Rather than requiring GCPs for georeferecing, the MSMS can achieve accurate mapping capabilities by recording the GPS position of the platform at the image exposure times while simultaneously providing the altitude and heading of the camera. The design goals for this project were to keep the system at a total weight of one kilogram, incorporate consumer grade sensors, and contain an independent power system and on-board data storage. These specifications were met and the MSMS proved to be a low cost, light weight, transportable way to provide navigation and 3D georeferenced data aboard unmanned vehicles.

1.1.6 Current Study

From the studies described above, it is apparent that SfM computer vision coupled with UAV-based aerial photography is showing an increasing demand due to its accessibility and versatility (Travelletti et al., 2012, Mancini et al., 2013). These case studies and research projects have proven the value of UAVs in their ability to obtain information and assist with problems

that would otherwise go unsolved. They allow researchers to access unsafe sites while remaining affordable and reliable. Their applications and the way in which they obtain data is considerable as is their contribution to the academic and commercial industries.

This thesis is the focus of a study using UAVs with aerial imagery. While all of the previous case studies have determined a way to use UAVs in a specific application, none of them have evaluated modifications to the data collection and SfM workflow to measure the impact on the resulting 3D model accuracy. The study described in this thesis provides a detailed analysis of the accuracy that is obtainable through the use of UAVs and aerial imagery. All of the different applications described above require different levels of accuracy and resolution depending on many factors including; scope of the project, research objectives, and area of study. The purpose of this study was to understand how model accuracy could be affected by modifying the type of data collected from the field and/or by modifying the SfM workflow. To accomplish this, several models were built using SfM technology and compared against a reference LiDAR scan of the site to determine how accurate each model was. Each digital reconstruction model had different processing parameters applied to it, requiring varying amounts of computer processing time in addition to man hours put in to the models. Knowing this information can help future researchers determine the amount of time it will take to get the desired amount of accuracy and resolution for a specified project.

In reviewing the available literature, a study that investigates the impact to model accuracy by varying the SfM inputs and/or workflow has not been previously performed. This type of analysis can be useful for any application as it examines how GCPs, processing quality, and GPS-tagged imagery can affect the accuracy of a model and the time it took to achieve that accuracy. The lack of guidance in the current literature on this topic can lead to confusion among

engineers and scientists as they try to detect changes and anomalies within their DTMs. Without knowing how much accuracy they can achieve, engineers and scientists will not know what workflow to execute to obtain a desired level of accuracy. This can lead to time being wasted on unnecessary processing steps and field work. This study will provide guidelines on how to achieve the desired level of accuracy in a 3D digital terrain model. With this knowledge, time and money can be saved on UAV projects if the proper workflow is determined in advance.

2 METHODOLOGY

The objective of this study was to quantify the accuracy of 3D digital point cloud models when different workflows and processing parameters are applied. To accomplish this, aerial imagery was collected using a helicopter UAV and a digital single lens reflex camera. The models were compared to a reference terrestrial LiDAR scan taken at the site which was assumed to be ground truth. This study was conducted at a landslide in the city of North Salt Lake, Utah in May of 2015. In addition to collecting photos at the site, GCPs were established and surveyed to be georeferenced to some of the models during processing. Using GCPs was one of the ways in which the models were altered and compared. There were three other factors that were tested against the ground truth including; camera GPS, processing quality, and the process of masking. Using various combinations of these parameters, 16 total models were created from 700 photos and compared to the LiDAR scan provided. The models were created using the computer vision software, Agisoft Photoscan and compared against the LiDAR using Cloud Compare. The time required to create each model was recorded in addition to the accuracy. The purpose of this method is to isolate and identify how different parameters contribute to the accuracy of a model. This in turn will reveal how much time and what combination of processing techniques is required to achieve a certain level of accuracy. The following sections explain the various ways in which each model was created and evaluated for accuracy, beginning with the capturing of the photos.

2.1 Site History

The site used for this study is located in the city of North Salt Lake, Utah. At this site a landslide occurred at about 6:00 a.m. on the morning of August 5th, 2014. The slope had originally been a gravel pit in the 1990s, but has since been reclaimed, engineered, and developed into a subdivision. When the failure occurred, it resulted in a 60 foot high main scarp above a landslide mass measuring 500 feet in width and length. This mass of soil and gravel moved downhill several dozen feet. Fortunately, no one was injured from this catastrophic failure and it only damaged one house beyond repair. It is estimated that the volume of the landslide is about 300,000 to 400,000 cubic yards, assuming a depth of between 30-50 feet. The pre-slide slope had a local relief of about 200 feet and an average grade of approximately 45 percent. It is still unclear to geologists and developers as to what caused this failure in the first place although there have been several speculations surrounding the events (Beukelman, 2014). The following image, Figure 2-1, shows the slide on the day it occurred.

As mentioned previously, many researchers have used landslides as their area of focus when using UAVs and remote sensors. The appealing aspect of landslides is that they can be studied over time and compared, allowing researchers to detect change in movement. While a change detection was not performed on this particular set of data, it is a possibility for further research. This data was used not to determine characteristics about a particular site but to gain further understanding of the UAVs and post-data collection processes themselves. This site was used in conjunction with that research purpose in addition to providing valuable data from the landslide. This particular study does not attempt to identify the cause of this failure, rather, the site is being used as a part of the study because of its geotechnical significance.

Figure 2-1: North Salt Lake Landslide (Beukelman, 2014)

2.2 Hardware

2.2.1 UAV

The UAV chosen for this study was the Align 800, displayed in Figure 2-2 which is an unmanned helicopter with a wingspan of 6ft. There are several advantages to using this piece of equipment over other aircraft. The helicopter can carry more weight than most UAVs. With all of the equipment required for this study, the weight of the payload totaled 19.5 pounds. This large load is one reason why the helicopter was selected. Another advantage to using the Align 800 is the stability it exhibits in the presence of precarious weather conditions. The slope at which the landslide is located experiences strong winds and the helicopter was able to fly and

remain stable throughout the field testing. The helicopter UAV is one of the most stable aircrafts available because it has a single blade instead of multiple. This is especially important for the photos to ensure that they are taken from a stable platform so as not to incur any image blur. The total flight time for the helicopter was 15-18 minutes and each flight lasted approximately 14 minutes. Two six-cell lithium-ion polymer batteries were used for each flight, totaling approximately five pounds. The pilot kept the aircraft at an average altitude of 50-100 feet above the face of the slide and a constant speed of approximately 5 mph.

The UAV was equipped with an Align G3 gimbal and GoPro camera (Figure 2-3 and Figure 1-1) to serve as the first person viewer (FPV) through which the field of vision of the UAV could be monitored. The gimbal, which held the sensor and the GoPro, had a separate transmitter, receiver, and battery source than the UAV and could therefore be remotely operated from the ground by a separate pilot. Video feed from the GoPro gave a representation of what the sensor was seeing through its lens. This live footage was fed directly to a monitor which could be seen by the secondary operator.

Figure 2-2: Align 800 Helicopter UAV

Figure 2-3: Align G3 Gimbal

2.2.2 Camera

The sensor that captured the imagery for this study was the Nikon D7100 DSLR camera equipped with a 35 mm lens, as shown in Figure 2-4. This camera features a 23.5mm by 15.6mm DX-format sensor capable of capturing images at resolutions of 24.1 megapixels (MP) and was set to a timer that captured a photo every three seconds while in the air. A default auto setting was chosen to take the pictures. This allowed for the photography to be as automated as possible while in flight. Taking high resolution photos was an important factor in this research study so high quality models could be produced which is why this camera was selected. While NEF images were captured with the camera originally, they were later converted to a TIFF format. Capturing photos in a NEF format is the default way for the Nikon to obtain raw image data. The lens used in this study was a Nikon AF-S Nikkor 35mm 1:1.8G. This lightweight, fixed-focal length lens has a large aperture, and it does not generate any wide-angle or telephoto distortion.

Figure 2-4: Nikon D7100 DSLR Camera

2.2.3 Computer

The computer used for this study was custom built to have enough processing power and capability to create all sixteen of the digital terrain models. Creating all of the models on the same computer was crucial to this study in order to maintain consistency. With enough processing power, the models were able to be developed in a timely manner as well as be compared against the LiDAR with limited problems within the hardware. Each model contained millions of points and massive amounts of data, ranging anywhere from 2-6 gigabytes of information per model. To ensure that the machine was able to handle the processing tasks, each component was carefully selected in the construction of the computer. The computer contained two Intel Xeon CPU E5-2680 v2 2.80GHz processors on a 64-bit operating system running Windows 8 with 256 GB of RAM. Having this much operating power allowed for a smooth workflow and easy manipulation of the data.

2.3 Software

The various types of software used in this project were chosen based on recommendations from industry and academia. Software that was mentioned repeatedly across several different articles was used to import, process, and compare the data. The following section describes in detail the three different software used and what purpose and function they served.

2.3.1 Agisoft Photoscan

Agisoft Photoscan was the software used to create the 3D terrain models. This is a software that performs photogrammetric processing of 2D images to create digital 3D terrain models using SfM algorithms. Throughout various studies performed, Agisoft has been the preferred tool in creating 3D models because of the accuracy and quality it produces. Agisoft was chosen to perform the bulk of the processing work in this study as well because of its robustness, reasonable price, workflow flexibility, and wide use in the academic literature. There are 2 main stages that comprise the model construction in Agisoft. The first stage is the alignment of the photos. During this step, common features are identified in the pictures and matched up. The position and angle of the photo when it was taken is also factored into this process. As a result, a sparse cloud is formed. This is a cloud containing thousands of points, sparsely distributed, that resemble the basic shape of the terrain. Because it is only a sparse cloud, it bears a rough semblance to the actual terrain while still maintaining general photo positions. The next step, the creation of the dense cloud, uses the sparse cloud and camera positions to create a much bigger, denser point cloud with depth information for each camera. This point cloud can contain up to 10 times as many points as the sparse cloud and therefore provides a much clearer, finished model.

2.3.2 Cloud Compare

Cloud Compare version 2.6.3 (Girardeau-Montaut, 2015) is an open source 3D point cloud and mesh processing software. It has the capability to manipulate large data sets and point clouds that contain millions of points. Just as the name suggests, its main function is to compare point clouds of data to one another. It can compare and detect changes across an entire point cloud or a small subsample of a cloud. An Iterative Closest Point (ICP) algorithm built into the software is used to compare two clouds. This algorithm keeps one point cloud fixed as the reference cloud and the other one, referred to as the source cloud, is altered to best align with and match the reference. For each point in the source cloud, the closest point in the reference cloud is located. After this closest point is located, the algorithm transforms the source point using a mean squared error function that provides the best alignment to the matching points. From these comparisons, many statistics can be computed based on the distance between the point clouds. The particular statistics and metrics used for this study will be presented in the "Results" section.

2.3.3 Xn Convert

Xn Convert version 1.72 is a software tool used to convert and edit batches of images across different platforms. It can alter the metadata of an image and changes the file type depending on the requirements of the software using the photos.

2.4 Different Parameters

This study was designed to test all parameters equally so comparisons would be objective. Table 2-1 below shows which combinations of parameters were input to each of the 16 models and the following sections describe how each parameter was altered to meet the needs of this study.

Table 2-1: Study Matrix Naming Scheme

	No GPS		Ground Control		Camera GPS		Ground Control and Camera GPS	
	No Masking	Masking	No Masking	Masking	No Masking	Masking	No Masking	Masking
Quarter Res (6MP)	1	2	3	4	5	6	7	8
Half Res (12MP)	9	10	11	12	13	14	15	16

2.4.1 GCPs

In reviewing the current literature, it was observed that several experiments instituted GCPs within their data. The advantages of establishing GCPs are very prevalent in the findings, as explained previously. While providing a way to georeference and improve the accuracy of digital 3D models, GCPs also have disadvantages. Marking and surveying GCPs can, at times, be difficult and dangerous given the hazardous conditions that occur in most sites. It may not always be a plausible option to incorporate GCPs into a model because of the potential danger that can come when exploring and surveying a site. Before a project can begin, researchers should determine if it is worth it to establish GCPs and if so, what are the risks and rewards that can come from them. The process of creating, positioning, and surveying GCPs is time consuming and therefore, more costly.

This study of the North Salt Lake landslide incorporated GCPs into eight of the models. The GCP markers were created before traveling to the site and distributed around the landslide based on the judgment of the researchers. In placing the GCP markers, the objective was to space them evenly around the slide to ensure complete coverage and equal distance between each point. To create the GCP markers, aluminum plates measuring 12 inches in diameter were spray painted a bright orange color so they would be easy to identify in the aerial photos. Figure 2-5 shows an aerial picture containing GCP markers which can be identified by the orange spots.

Each plate was painted with a number from 1-12 and punctured with a hole in the middle to allow for a stake to anchor the plate into the ground, that can be seen in Figure 2-6. The 12 GCP markers placed around the landslide were surveyed using a Topcon GR-3 GPS system, complete with a receiver and handheld controller, shown in Figure 2-7. If a plate was visible in a photo, it was manually tagged and referenced to the corresponding GPS coordinate. This process took up a significant amount of time. The time required to place and survey the GCP markers in addition to the process of marking the GCPs in the individual photos took about five additional hours. The analysis of the models with GCPs incorporated into them will reveal if this time was worth the effort. From the results the accuracy will be analyzed to determine whether or not the GCPs contributed to an increase in accuracy. If that is the case, researchers can then determine if that increase in accuracy is worth the time and money that would be spent on including GCPs in a digital terrain model.

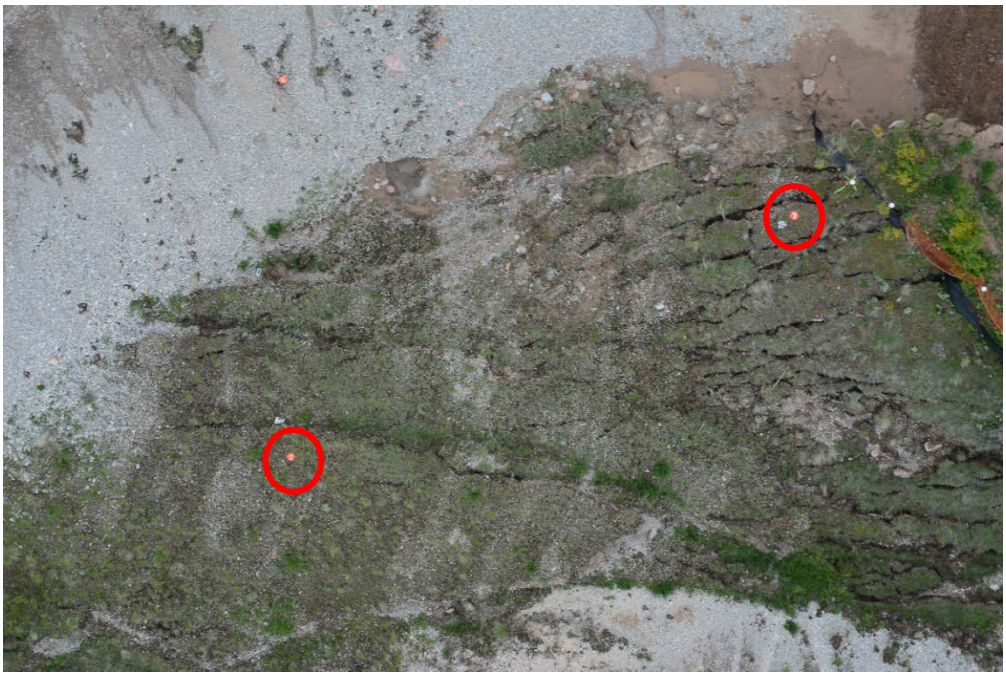

Figure 2-5: Aerial Photos of GCPs

Figure 2-6: GCP Marker Used for This Study

Figure 2-7: Topcon GR-3 Survey Equipment

2.4.2 Camera GPS

While georeferencing the digital reconstructions of a site using GCPs is a popular option, there is another way to add geographic information to a photo data set. Attaching a GPS directly to the sensor can provide a wealth of information that is attached to each photo. For this particular study, a Geotagger Pro2 Solmeta (Figure 2-8) GPS system was used to geotag the photos. The Geotagger unit includes a 3-axis compass and 3-axis acceleration sensors, allowing it to take accurate readings even when it is tilted at various angles. This GPS unit provided the latitude and longitude coordinates for each photo as it was taken. This reference point information is used by the computer vision software to better align the photos. The SfM algorithm built into the computer vision software takes the geotagged data and can identify where each photo was taken from.

Figure 2-8: Geotagger Pro 2 Solmeta

This method is easier and less time consuming than adding GCPs to a model as it only requires the user to simply attach the unit to the camera and it automatically records data as each

picture is taken. Four of the models will use only the GPS coordinates collected from the camera and four different models will incorporate the camera GPS as well as the GCPs. The results of this study will determine if this method also provides more accurate models than using GCPs.

2.4.3 Processing Quality

The computer vision software, Agisoft Photoscan, which stitches the photos together to create 3D models processes the pictures on different setting qualities (Agisoft LLC, 2011). When the points from the photographs are matched up, a sparse cloud is created. The settings for the creation of the sparse cloud were kept constant for each model. However, the settings for building the dense cloud were altered. A dense cloud is created after the sparse cloud and it can be processed under a medium or a high quality. The quality setting determines what resolution of the photos is used to create the dense cloud. More discussion on the creation of the dense cloud will be included in the upcoming section entitled, "Software."

When changing the settings on the construction of the dense cloud, the options include "Low", "Medium", "High", and "Ultra High." For the purposes of this study and to keep the processing time within a reasonable range, the "Medium" and "High" settings were chosen to be tested and compared against each other. The "Low" setting was omitted because in the past, it has produced models that are not high enough quality to be used by researchers. In looking at the "Ultra High" setting, it was determined that this setting would take too long to process the photos and create a dense cloud. According to the Agisoft PhotoScan user manual (Agisoft LLC, 2011), the "Higher quality settings can be used to obtain more detailed and accurate geometry, but require longer time for processing." This difference in processing time occurs because of the resolution of the photo that the program enables to create the point cloud. When enacting the medium setting, Agisoft only uses a quarter of the resolution of the photos. However, the high

setting uses half of the resolution, allowing it to pick up more points and features in each photo. Because it uses more resolution, it requires more time than the medium setting.

2.4.4 Masking

When preparing a set of photos to be processed, there is an option to alter what is and is not processed within each individual photo. The process of masking allows the user to crop out specific areas in a photo that can be unclear to the program or unnecessary to the reconstruction of the scene. Including masking on a photoset is the last factor that was adjusted in the study of comparing time and accuracy. Eight of the models included masking and the other eight did not have masking applied, meaning the entire image was used for each photo.

Masking photos requires at least two hours of additional time by the user. The process involves examining each of the 700 photos used for this study and identifying areas in each image that do not need to be included in the final digital model. These areas are categorized as unusable because they are redundant or do not have anything to add to the reconstruction because they are not within the area of interest. Once these areas are identified, the user highlights them individually on a photo and the Agisoft program will not include them in the creation of the point cloud. Determining which areas to exclude from the images is at the user's discretion and is a completely subjective process. Oftentimes, sections that include the sky or other distant objects that are not part of the study site are masked out. Not every photo needs the masking process applied to it. If every part of the image is relevant, none of it will need to be omitted through masking. While not every photo needs to be masked, every photo needs to be inspected to determine if masking is applicable which involves extra time on the part of the researcher. The outcome of this study will determine if the time spent on masking will improve the accuracy enough to justify the cost of the extra effort spent. Figure 2-9 illustrates the masking

process of a raw image that is cropped out where the unwanted area is turned gray and the final product, shown in the last image, does not include that specified area.

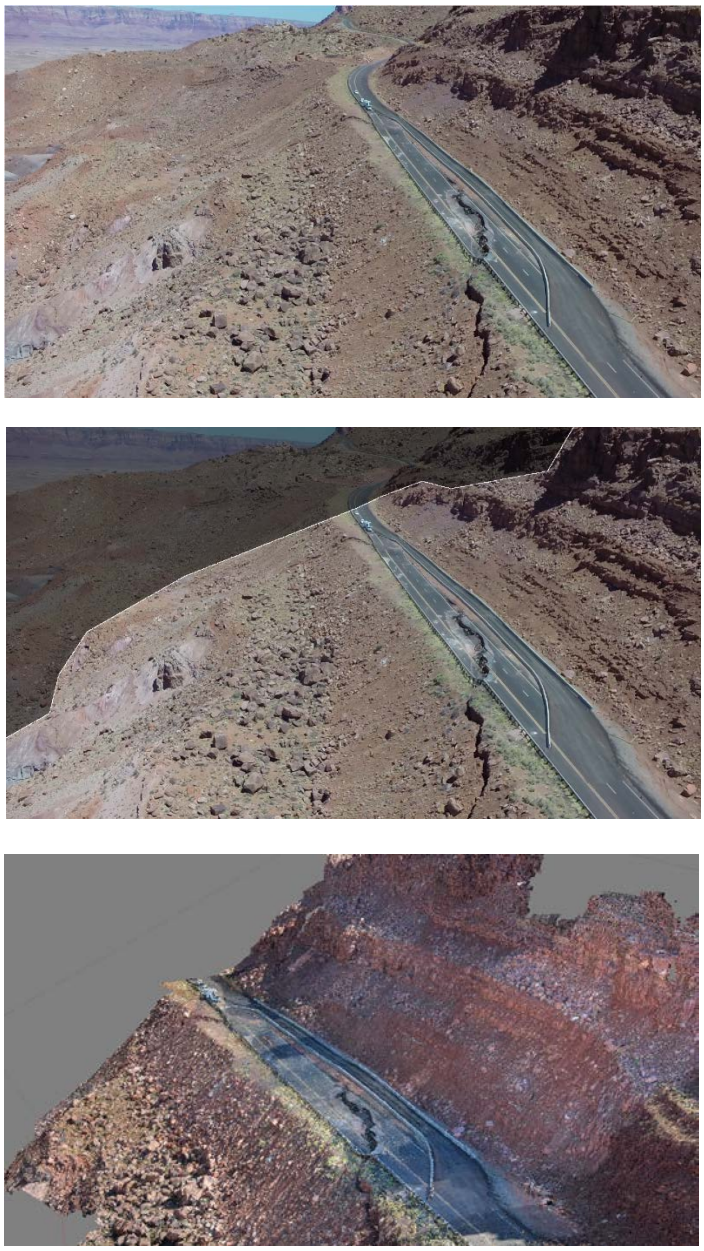

Figure 2-9: Masking Process

2.5 Workflow

2.5.1 Collecting the Data

The data for this study was obtained over a two day period in May of 2015. First, the GCP markers were set up around the landslide and surveyed. They were placed as evenly as possible to ensure full coverage of the site with about 100 feet between each one on all sides. As mentioned previously, 12 of them were made and numbered so they were easy to identify in the aerial imagery. The GCPs were established prior to the flights to ensure that they would appear in the photos.

The helicopter UAV, equipped with the camera mounted to a stabilizing gimbal, was flown for a total of seven flights during which 1,500 photos were taken. The camera was programmed to capture one photo every three seconds as it travelled around the site. Seven flights were conducted to ensure adequate aerial coverage, as determined by the pilot and fellow researchers. Each flight lasted about 15 minutes due to the limiting factor of the battery power. While one pair of batteries was powering the helicopter, two backup pairs of batteries were charging to make certain that batteries would be immediately available for subsequent flights. The pilot as well as the other researchers planned the flights according to the areas of greatest significance on the landslide as well as to obtain enough overlap in the photos. For the purposes of the comparisons in this study, the area of greatest significance included the main scarp of the landslide, as this was the area that would be compared against ground truth. Once the flight was planned from the ground, the pilot manually controlled the aircraft around the flight path using his best judgment on obtaining the proper imagery overlap. The UAV was flown above the landslide at an average height of about 50-100 feet at an average speed of 5 mph.

Attaching the camera to a moveable gimbal allowed for it to be remotely controlled by a separate operator from the ground. Using FPV footage from the GoPro as a guide, the gimbal was maneuvered to be directed at the area of interest. The gimbal operator could rotate the camera about three different axes to position the lens toward the slide. Using a gimbal was advantageous to providing a method for capturing clear, precise images, free of blur.

After each flight was completed, the images taken during that time were downloaded to a laptop from the camera's SD card. This process was necessary for two reasons. It allowed for the SD card to be cleared of any data and reused for each flight, and it created a way for the pictures to be examined after each flight to ensure that they were capturing the desired areas. This was repeated for each of the seven flights. Once the photos for one flight had been captured, the UAV was prepared for the next flight. This involved changing the batteries on the UAV, camera, and gimbal as needed and clearing the SD card of all the previous flight's pictures.

During the course of this field study, safety measures were enacted to keep the researchers and surrounding residents protected. Before each flight, a 20 foot radius around the helicopter was cleared and the pilot took extra caution in taking off and landing to ensure that no accidents occurred. While in the air, the UAV was constantly monitored by maintaining line-of-sight vision by several people on the research team so its location was always known and crashes were avoided. The pilot had adequate amounts of training and practice and was able to maintain control of the copter at all times with the assistance of spotters, as needed.

2.5.2 Establishing Ground Truth

To be able to compare the models and determine their accuracy, industry-standard ground truth needed to be established at the site. This was accomplished by obtaining a terrestrial LiDAR scan of the landslide. This LiDAR was taken using a FARO Focus 330 unit (Figure

2-10) which claims an accuracy of +/-2mm at ranges of 130 m and 330 m, respectively. This level of accuracy is so close to zero, it is assumed to be ground truth for this study. The terrestrial scanning of the site was done by professional land surveyors, separate from the university. Their process began by mapping out a series of predetermined positions across the slide designed to promote maximum coverage. Several spherical Styrofoam targets with diameter ranging from 150mm to 200mm were placed in the scan vicinity to facilitate object registration. In total, 27 separate TLS scans were made over a period of two days and 32 total man hours between two surveyors. This scanning was carried out on the same days the flights were done to maintain consistency and reduce discrepancies between the models. Registration of the TLS scans was performed using AutoDesk ReCap software, unifying the scans into a single 3D point cloud model. This model was converted into an .E57 file format, a compressed file compatible with Cloud Compare. A screenshot of the finished LiDAR point cloud can be seen in Figure 2-11.

Figure 2-10: FARO Focus 330 LiDAR Scanner

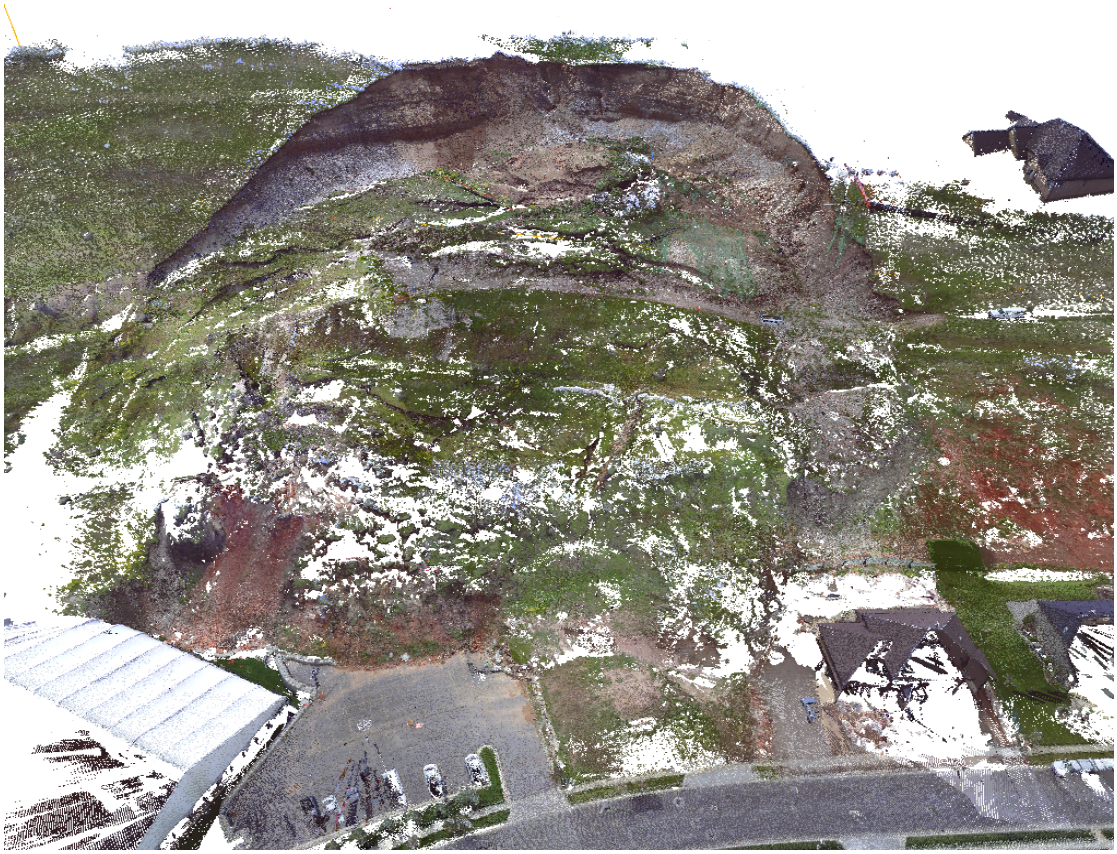

Figure 2-11: Terrestrial LiDAR Point Cloud Model

2.5.3 Pre-processing

Once the data had been gathered from the site, the pre-processing work began. Before the SfM algorithm could run and create the digital 3D model, the pictures had to be carefully selected and prepared. The preparation of the photos was done based on the recommendations found in the literature as well as those suggested in the Agisoft Photoscan user manual.

The helicopter UAV was able to capture roughly 1500 photos from the site. Prior to the photos being uploaded into the Agisoft software, they were converted from a NEF format into a TIFF format. This had to be done because the Agisoft software will accept a TIFF format and not a NEF image format. A TIFF format was preferred for this project because it contains the raw image without any compression or unwanted noise being introduced. The photos were captured

initially in the NEF format because this is the default format for capturing raw images with the Nikon camera. The Xn Convert software was used to convert the images from one type of raw image to another in order to meet the needs of Agisoft Photoscan.

From these photos, the best ones were selected to be included in the 3D terrain model. Many of the pictures were redundant, irrelevant or unusable due to image blur. Reducing the photo set required the researcher to look through each of the pictures and determine which were worth keeping. This process was rather arbitrary and at the discretion of the researcher. If an image was too blurry or did not contain parts of the area of interest, it was discarded. During the flights, several sequential images were often captured that looked very similar. Any of these redundancies were excluded and only a couple pictures from a string of repetitive photos remained.

The Agisoft program contains a function that will estimate the image quality of a photo on a scale from 0 to 1. An image receiving a score between 0-0.5 was discarded. The estimation of image quality was done based on the clearness of the photo. If an image was blurry or vague, a lower quality score was given by the software. After applying this feature to all the photos, about 200 fell below the desired quality level and consequently, were deleted.

After deleting the unwanted pictures subjectively or using the image quality estimator, 700 photos were selected to move to the next stage of pre-processing. It was advantageous to capture more photos than were needed to ensure that the coverage of the site was complete. While the process of narrowing down the photo set required 2 additional hours of time, it was preferable to have more images than were necessary than to have to make a return visit to gather missing data.

The next step in pre-processing is applying masking and/or geotagging the GCPs within the individual photos. Half of the models were masked and half of them had georeferenced GCPs. Masking and georeferencing each required an additional two hours of time from the researcher. These steps are so time consuming because they involve looking at every photo and determining if that photo needs masking or geotagging, as described previously. All of these steps were completed in Agisoft using various commands and functions. The masking tool was used to isolate and remove unwanted areas. Geotagging the GCPs was accomplished using the "Create Marker" tool that placed a symbol with an assigned number and coordinate on the user-identified GCP. The camera GPS did not need to be added to the photos manually, rather, the metadata attached to each photo was simply imported if the specific model required GPS coordinates from the camera.

2.5.4 Processing

After all of the parameters were applied to each specific model, the workflow of processing the photos within Agisoft began. The first step, creating the sparse cloud was done using the "Align Images" tool. All of the default inputs were used during this stage as follows:

- Accuracy: High
- Pair Preselection: Disabled

Once the sparse cloud was completed, the dense cloud was completed in the Agisoft workflow. Figure 2-12 demonstrates the difference between the sparse cloud and the dense cloud. The sparse cloud has several holes in the model and is a lower quality, aesthetically. This is the reason the dense cloud was the point cloud used in the model comparisons against LiDAR. The selected accuracy of the dense cloud was "Medium" for half of the models and "High" for the other half. During each step of the model processing, the time required to complete it was

recorded to be included in the results. Completing the dense cloud then allowed for each cloud to be exported to a .ply file that could be analyzed in Cloud compare and compared with the TLS model.

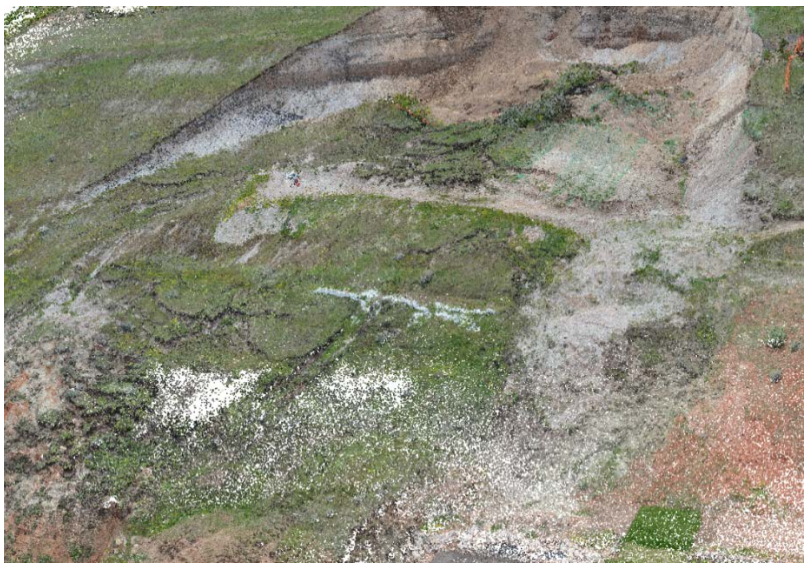

(a)

(b)

Figure 2-12: Agisoft Point Clouds – (a) Sparse Cloud (b) Dense Cloud

2.5.5 Comparing the Data Sets

The final step of this study was comparing the 3D models against the ground truth LiDAR models. For each individual model, a separate comparison had to be made. Comparing the data sets was a time consuming process and required several iterations to obtain usable information. The final workflow for data comparisons was carried out in Cloud Compare. Every comparison required the designation of a reference cloud that remains stationary and a source cloud that is transformed to best match the reference cloud. The TLS cloud was always identified as the reference cloud, with the Agisoft models labeled as the source cloud. The first step required a manual alignment of the two clouds before the ICP algorithm could be run. For this step, three points that appeared in each cloud were manually selected and identified by the user. It should be noted that these identical points were chosen manually and were therefore at the discretion of the researcher. Next, the program performed a transformation by rotating and scaling the source cloud to match it up with the reference cloud based on these selected points. These aligned clouds were then segmented off into 10 smaller sections taken from the main face of the landslide. The area chosen from the landslide models was picked because of its significance in making comparisons for a practical application such as monitoring displacement on the face of a landslide. After each of the ten pieces was partitioned off, as seen in Figure 2-13, the ICP algorithm was run. As described above, this function in Cloud Compare matched the two clouds based on the closest point between the source and the reference. The output of this process is a mean accuracy, or, the average distance between all the points. This was the number used to quantify the accuracy of the digitally reconstructed SfM models. Segmenting and selecting these 10 smaller sections was again up to the judgment of the user and was done to obtain an average accuracy. Performing the ICP algorithm over the entire slide produced

erroneous results and the best way to combat that was to take an average reading over several smaller sections of points. This meant that for each of the 16 models, 10 different comparisons had to be made. The average of the mean distance from all 10 clouds was used in the results as a measure of the accuracy.

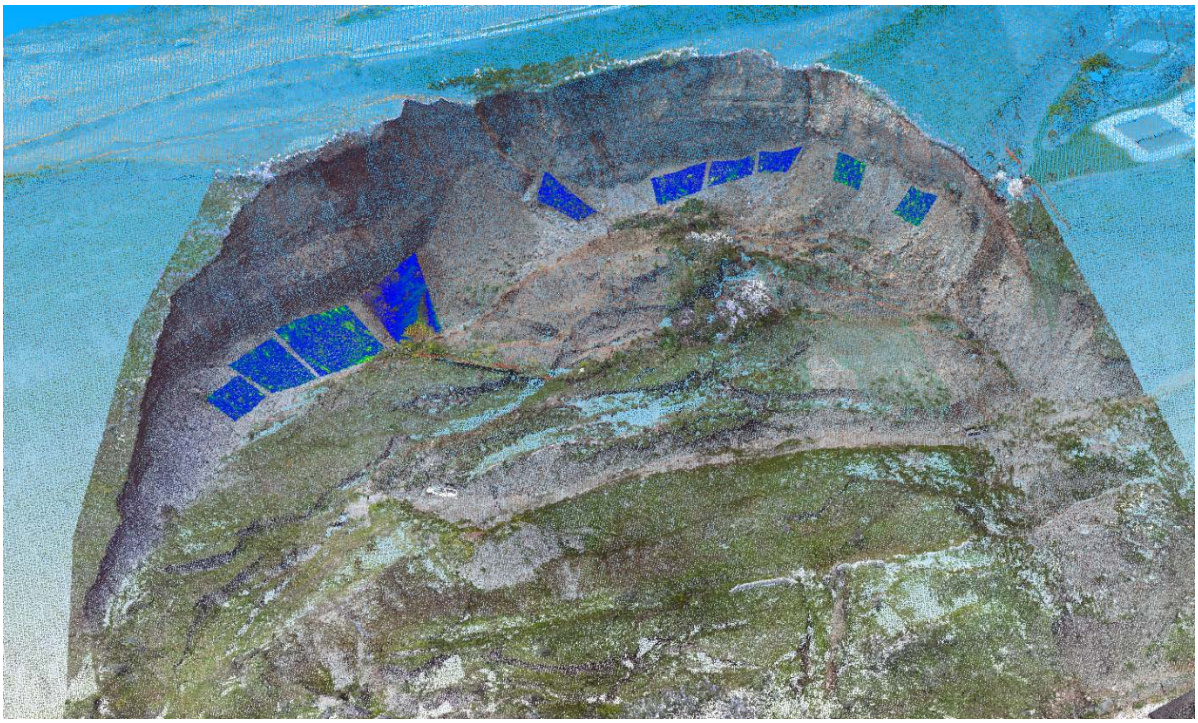

Figure 2-13: Segmented Comparisons Along Face of Landslide

The following images in Figure 2-14 are intended to highlight the difference between the TLS model and a SfM model used for comparisons. The TLS model has several holes and areas where there are no points associated with them. This most likely occurred because of the nature in which this data was collected. Trekking around the terrain on foot with a scanner that was mounted on the ground made it difficult to see and acquire points from every corner of the

landslide. Gathering photos from an aerial perspective allowed the SfM models to have much more coverage than the TLS model, as seen in these pictures.

(a)

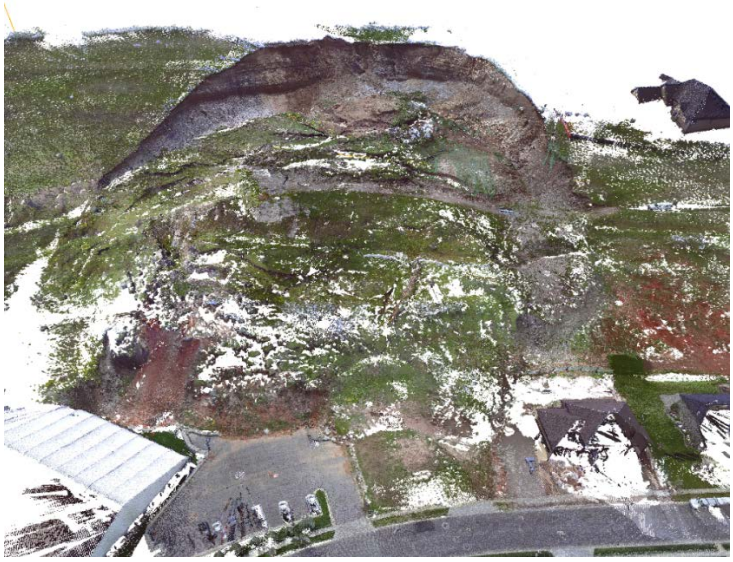

(b)

Figure 2-14: Model Comparisons – (a) TLS Model (b) SfM Model

3 RESULTS

3.1 Accuracy

The following figure, Table 3-1, shows the quantified accuracies of each of the sixteen models. These numbers, displayed in centimeters, represent the average distance error between the points after the ICP algorithm aligned the two models. The lower the distance error, the more accurate the SfM model. After the two clouds were aligned, a calculated distance value was given to each point. Also calculated in Cloud Compare was the average of all these distances. This table is the average of all those values taken from 10 different sections across the landslide, as explained in the Methodology section of this report. The averages from each of the ten different sections can be found Appendix B.

Table 3-1: Accuracy of Model Comparisons

	No GPS		**Ground Control**		**Camera GPS**		**Ground Control and Camera GPS**	
	No Masking	**Masking**	**No Masking**	**Masking**	**No Masking**	**Masking**	**No Masking**	**Masking**
Quarter Res (6MP)	1.78 cm	1.71 cm	1.36 cm	1.30 cm	1.80 cm	1.85 cm	1.86 cm	1.41 cm
Half Res (12MP)	1.38 cm	1.37 cm	1.15 cm	1.21 cm	1.35 cm	1.30 cm	1.15 cm	1.29 cm

The objective of this study was not only to quantify accuracy of SfM models but to evaluate that accuracy based on the amount of time it took to create the model. Table 3-2

presents the times, in hours, that were required to finish the models so this research objective could be accomplished. These times include not only the man hours that were put into the creation of a model but the computer processing time. The man hours consist of all the time contributed in the field as well as pre and post-processing of the data. A complete breakdown of the time contribution for each stage of the model creation can be found in the Appendix A.

Table 3-2: Time for Model Creation

	No GPS		Ground Control		Camera GPS		Ground Control and Camera GPS	
	No Masking	**Masking**	**No Masking**	**Masking**	**No Masking**	**Masking**	**No Masking**	**Masking**
Quarter Res (6MP)	13.0 hrs	14.9 hrs	25.1 hrs	20.6 hrs	11.5 hrs	13.8 hrs	16.7 hrs	20.7 hrs
Half Res (12MP)	116.4 hrs	39.3 hrs	64.6 hrs	59.5 hrs	37.5 hrs	46.0 hrs	52.2 hrs	81.5 hrs

In looking at the amount of time versus the accuracy that was obtained, there are many trends that are observed. These trends, as interpreted by the student researcher, are intended to give insight as to how to obtain the most accurate SfM models in the smallest amount of time. The following sections will explain the contribution of each parameter to the overall accuracy.

3.1.1 Georeferencing

Ground control points were used in half of the models. Four of the 16 models relied solely on GCPs to georeference the model and the other four were georeferenced with the camera GPS in addition to GCPs. Including GCPs in the model increased the time in the field and during the pre-processing stage by a total of 4 hours. In comparing the total time of the models, 3 out of the 4 models that had GCPs took longer to process than the models that had no GCPs. On average, the time to create a model with GCPs increased by about 35%. The reason

for this significant increase in time is not only the physical process of placing and surveying the GCPs but also the computer processing time. While the addition of GCPs does assist the Agisoft program with aligning the photos by giving them more geotagged data, it also demands more time. This is potentially due to the added information that the software has to incorporate when it aligns the pictures.

While adding GCPs to a model does increase the processing time, it also increases the accuracy. Every model that had GCPs was more accurate than those without. This increase in accuracy was, on average, about 19%. Throughout the reviewed literature, researchers have found that GCPs increase the accuracy of their models and that trend is continued in this study. This occurs because the models became referenced to a real world coordinate system, much like the TLS scans they were compared to.

The GPS coordinates acquired from the camera were added to half of the models. Similar to the GCPs, four of the models had camera GPS alone and four of the models had camera GPS as well as GCPs. The total processing time for models with camera GPS was about 17% less than the time it took to create the models that did not have camera GPS. It is possible that this decrease in time can be attributed to the camera GPS making it easier for Agisoft to align the photos. In analyzing the accuracy that was obtained by integrating camera GPS, these models were, on average, 0.51% more accurate than their counterparts with no camera GPS. While this is not a significant increase in accuracy, it does require less time to produce these models.

Four of the models combined camera GPS and GCPs into the final product. Compared to the models with no georeferencing at all, these four took about 30% more time to complete than the models containing no georeferencing. It is interesting to note that in addition to these models, the models with strictly GCPs also required more time to complete than the models with no

georeferencing, while the models using only camera GPS took less time to complete. In observing the accuracy of the models containing both methods of georeferencing, it can be seen that they are, on average, 8.9% more accurate than the models without.

Table 3-4 provides a summary of these results that clearly display the increase or decrease in time and accuracy that each type of georeferenced model produced when compared against the models that have no georeferencing. Using this data, in conjunction with the following sections of results, an informed decision can be made about which types of models will give the best accuracy. From solely looking at this table, the GCPs gave the best increase in accuracy but also involved more time. Models employing camera GPS used the least amount of time but did not return a significant amount of accuracy improvement. The accuracy of a model with both GCPs and camera GPS combined is higher than one that uses camera GPS alone and lower than a model with only GCPs. This information suggests that incorporating camera GPS is detrimental to a model's accuracy when combined with GCPs. These results could depend on the accuracy of the GPS and how well the SfM algorithm is able to align photos with two sets of geotagged data, each relying on different equipment.

3.1.2 Processing Quality

Changing the processing quality on a model can cause a significant difference in time and accuracy, as exhibited in Table 3-1 and Table 3-2. Half of the models were processed on the medium setting and the other half were on the high setting. It is a known fact, as revealed in previous literature, that processing a model on a higher quality will yield more accurate results but require longer time for processing. The question then becomes, how much more accurate can these models become from that increase in processing time?

The increase in time discussed in the reviewed literature and the Agisoft user manual can be seen in Table 3-2. Processing a model at a high quality versus a medium quality significantly increases the time by about 2.8 times. This needs to be taken into consideration when choosing a model quality, as this amount of time can potentially reduce productivity. Just as was foreseen by previous studies, the increase in processing quality did increase the accuracy in every instance. Averaging about a 21% rise in accuracy, with a maximum of 38%, the increase in quality showed a significant improvement when adjusted from medium to high. Another notable difference between medium and high models is the number of points in the dense cloud. On average, the models processed on the high quality had about 250 million points while the medium models had about 60 million points. Having almost four times more points is a contributing factor to the increased accuracy. The more points that are in a model, the more chance there is for a point on the reference cloud to match up with a point on the source cloud, therefore causing a higher accuracy calculation with the ICP algorithm. Figure 3-1 below shows a screenshot of a close up detail of a medium and a high point cloud for comparison. From looking at these two images, it can be observed that the medium quality has less detail and a fuzzier resolution than the high quality model.

Being able to obtain a notable increase in accuracy with this method can be very beneficial to any research objective, if a researcher is willing to dedicate the appropriate amount of time. This parameter is perhaps the most influential factor on the time and accuracy that a model will incur.

(a)

(b)

Figure 3-1: Close Up Detail of (a) Medium and (b) High SfM Point Clouds

3.1.3 Masking

Masking was implemented in half of the models while the remaining half were processed without it. The procedure of masking required more time on the part of the user in the initial stages of processing. It required an additional two hours to view all the photos and identify areas that needed to be masked out. Assessing the total time required, models with masking took longer to process in five out of the eight cases. Taking an average across all eight models, masking used up 5.7% more time than those models without masking.

Accuracy of models with masking appeared to be better than no masking in five out of the eight models. While five out of the eight models also required more time to complete, there was not a direct correlation between the increased time and the improved accuracy on each individual model. The average increase in accuracy among all eight models was 2.1%. This is not a considerable amount of improvement, however, considering the time increased by only 5.7%, the accuracy is reflected in that time increase.

3.2 Resolution

The resolution of the models was recorded as the average number of points located within a square meter. To accomplish this, an area was measured on a flat part of the model where there were limited gaps and holes and the amount of points was recorded in that area.

Table 3-3: Model Resolution

	No GPS		Ground Control		Camera GPS		Ground Control and Camera GPS	
	No Masking	**Masking**	**No Masking**	**Masking**	**No Masking**	**Masking**	**No Masking**	**Masking**
Quarter Res (6MP)	790 pts/m^2	731 pts/m^2	778 pts/m^2	785 pts/m^2	808 pts/m^2	728 pts/m^2	779 pts/m^2	701 pts/m^2
Half Res (12MP)	3081 pts/m^2	2249 pts/m^2	3224 pts/m^2	2960 pts/m^2	3162 pts/m^2	2200 pts/m^2	2603 pts/m^2	2052 pts/m^2

These results indicate that the resolution of the half resolution models is up to four times better than that of the medium resolution models. It is also interesting to note that the models without masking had a higher resolution than those with masking in almost every instance. In observing the difference in resolution of models with GPS data versus those without, there is not a strong correlation among the varying resolutions. Resolution is a god indicator of how many points are in a model and can be of use to researchers. However, a model with a higher resolution does not always mean that it will be more accurate.

The ground sampling distance of a model is the number that represents the average distance (as measured on the real world object) between the pixels in a photo. Photos taken from further away will have more area to cover with the same amount of pixels than a closer photo. The images in this study were taken at distances varying from 15 – 45 meters away. These distances gave a ground sampling distance range of 0.378 – 1.135 centimeters per pixel. This indicates that the photos taken at a distance of only 15 meters had an average of 0.378 cm between each pixel while those taken at the further distance of 45 meters had a ground sampling distance of 1.135 cm.

3.3 Chapter Summary

Summarized below, in Table 3-4, are the analyzed results from each parameter displayed as an increase or decrease in time and accuracy. The increase or decrease is determined as the change from implementing a certain parameter versus the models without that parameter. Making the change from high to medium quality, for instance, required 280% more time but gave the highest increase in accuracy. This table only provides a summary of the results and

should be used in conjunction with Table 3-1 and Table 3-2. These summarized results can help future researchers decide which parameters to incorporate into their digital terrain models based on the amount of time they want to devote and the level of accuracy they want to achieve.

Table 3-4: Quantitative Results Summary

	GCPs	Camera GPS	GCPs and Camera GPS	High Quality	Masking
Time	+35%	-17%	+30%	+280%	+5.7%
Accuracy	+19%	+0.51%	+8.9%	+21%	+2.1%

4 CONCLUSION/RECOMMENDATIONS

Many applications of UAVs have been studied and evaluated for their effectiveness over the past few years. The recent increase in popularity of UAVs among researchers has provided a lot of valuable resources and insight into the best methods and techniques for obtaining usable data from coupling remote sensing with UAVs. This study was unique in that it examined the change in accuracy that would occur when various SfM parameters were altered.

4.1 Conclusions

This study created a foundation of information about obtaining quantifiable results from digital terrain models made through the use of UAVs. Using this information and results, future researchers and students alike can determine what level of accuracy they can attain for the amount of time they want to dedicate to a digital terrain model. Some important observations about the SfM process, remote sensors, and employing UAVs in a research project came as a result of this research study. These include:

1. Using a UAV instead of LiDAR to monitor a site has several advantages. A UAV required less time to use than a commercial LiDAR unit. In comparing the models qualitatively, the SfM ones were much more complete with limited gaps and holes while the LiDAR model had several patches of missing data because of the difficult

nature of the terrain. The LiDAR model had more points in the cloud but not as evenly spread out as the UAV models. While the use of UAVs were advantageous for this and other previously mentioned studies, there are cases where using a LiDAR unit would be preferable.

2. When comparing the models to one another, comparing smaller segments and averaging them provided better results than comparing the entire models. After several iterations and trials, this was found to be the best way to compare the models. It is possible that the ICP algorithm contributes to this.
3. The results obtained from this study show that an average 66.7% increase in time will lead to an average 10.3% increase in accuracy. The summary, presented in
4. Table 3-4, displays the precise numbers and these can be used by future researchers at their own discretion.
5. A model that has more points in it will not necessarily be more accurate. While a model may look better aesthetically than another, it does not mean it will be more or less accurate. It is possible that the points are distributed differently across two different models.
6. The results presented here are from one study and one site and were created to have as little inconsistencies as possible. However, many steps in the model comparisons were done manually and therefore introduced a small amount of variability. It was also assumed that the terrestrial LiDAR, which claimed to be accurate to within +/-2 mm by the manufacturer, was “ground truth.”

4.2 Recommendations for Future Research

The results found through this study can prove to be quite useful for future work and research. However, there is much more research that can expand on the ideas and results discussed in this report. This study was only conducted on one site with one type of platform. To verify or modify these results, future work could involve several different sites and UAVs and determine if that alters the accuracy of models in any way. It might also be of interest to study the resolution and density of the models and how that affects the accuracy. The distribution of points across a model could influence how accurate it is.

The method for comparing models was created by the researchers of this project and there could be better, simpler ways to perform this step. While the process presented here was quite arbitrary, a different study could be conducted to find a more systematic, consistent approach.

Future work can always be done on the application side of this project. Taking these results and applying them to a future study would make for an interesting experiment that could either confirm or refute these results.

REFERENCES

Agisoft LLC. (2011) *Agisoft PhotoScan User Manual*.; www.agisoft.ru.

Beukelman, Gregg. Parkway Drive Landslide, North Salt Lake. *Utah Geological Survey.* Utah Geological Survey, n.d. Web. 07 June 2016.

Buckley SJ, Howell J a., Enge HD, Kurz TH. (2008) Terrestrial laser scanning in geology: data acquisition, processing and accuracy considerations. *J Geol Soc London*.;165(3):625-638.

Chen S, Asce M, Rice C, Boyle C, Hauser E. (2011) Small-Format Aerial Photography for Highway- Bridge Monitoring. *J Perform Constr Facil*.;25(April):105-112.

Cooper AJ, Redman CA, Stoneham DM, Gonzalez LF, Etse VK. (2015) A dynamic navigation model for unmanned aircraft systems and an application to autonomous front-on environmental sensing and photography using low-cost sensor systems. *Sensors (Switzerland)*.;15(9):21537-21553.

Dobson RJ, Brooks C, Roussi C, Colling T. (2013) Developing an unpaved road assessment system for practical deployment with high-resolution optical data collection using a helicopter UAV. *2013 Int Conf Unmanned Aircr Syst ICUAS 2013 - Conf Proc*.:235-243.

d'Oleire-Oltmanns S, Marzolff I, Peter K, Ries J. (2012) Unmanned Aerial Vehicle (UAV) for Monitoring Soil Erosion in Morocco. *Remote Sens*.;4(12):3390-3416.

Ellenberg a., Branco L, Krick a., Bartoli I, Kontsos (2014) Use of Unmanned Aerial Vehicle for Quantitative Infrastructure Evaluation. *J Infrastruct Syst*.;21(3):04014054.

Harwin S, Lucieer A. (2012) Assessing the accuracy of georeferenced point clouds produced via multi-view stereopsis from Unmanned Aerial Vehicle (UAV) imagery. *Remote Sens*.;4(6):1573-1599.

Immerzeel WW, Kraaijenbrink PDA, Shea JM, et al. (2014) High-resolution monitoring of Himalayan glacier dynamics using unmanned aerial vehicles. *Remote Sens Environ*.;150.

Kersten TP, Lindstaedt M. (2012) Image-based low-cost systems for automatic 3D recording and modelling of archaeological finds and objects. *Lect Notes Comput Sci*

Koska B, Kremen T. (2013) The Combindation of Laser Scanning and Structure from Motion Technology for Creation of Accurate Exterior and Interior Orthophotos of St. Nicholas Baroque Chrich. *Int Arch Photogramm Remote Sens Spat Inf Sci*.;XL(February):25-26.

Li-Chee-Ming J. (2012) Development of a Low-Cost Mobile Stereometric Mapping System for Unmanned Vehicles. *ProQuest Diss Theses*.;MR90086(April):182.

Lucieer a., Jong SMD, Turner D. (2014) Mapping landslide displacements using Structure from Motion (SfM) and image correlation of multi-temporal UAV photography. *Prog Phys Geogr*.;38(1):97-116.

Mancini F, Dubbini M, Gattelli M, Stecchi F, Fabbri S, Gabbianelli G. (2013) Using unmanned aerial vehicles (UAV) for high-resolution reconstruction of topography: The structure from motion approach on coastal environments. *Remote Sens*.;5(12):6880-6898.

Matese A, Toscano P, Di Gennaro S, et al. (2015) Intercomparison of UAV, Aircraft and Satellite Remote Sensing Platforms for Precision Viticulture. *Remote Sens*.;7(3):2971-2990.

Niethammer U. (2010) UAV-based remote sensing of landslides. ... *Remote Sens* .... ;XXXVIII(2005):496-501.

Niethammer U, James MR, Rothmund S, Travelletti J, Joswig M. (2012) UAV-based remote sensing of the Super-Sauze landslide: Evaluation and results. *Eng Geol*.;128:2-11.

Nishar A, Richards S, Breen D, Robertson J, Breen B. (2016) Thermal infrared imaging of geothermal environments and by an unmanned aerial vehicle (UAV): A case study of the Wairakei – Tauhara geothermal field, Taupo, New Zealand. *Renew Energy*.;86:1256-1264.

Piermattei L, Carturan L, Guarnieri A. (2015) Use of terrestrial photogrammetry based on structure-from-motion for mass balance estimation of a small glacier in the Italian alps. *Earth Surf Process Landforms*.;1802(July):n/a - n/a.

Rathinam S, Kim ZW, Sengupta R. (2008) Vision-Based Monitoring of Locally Linear Structures Using an Unmanned Aerial Vehicle 1.;14(1):52-63.

Shahbazi M, Sohn G, Théau J, Menard P. (2015) Development and Evaluation of a UAV-Photogrammetry System for Precise 3D Environmental Modeling. *Sensors (Basel)*.;15(11):27493-27524.

Stumpf A, Malet JP, Kerle N, Niethammer U, Rothmund S. (2013) Image-based mapping of surface fissures for the investigation of landslide dynamics. *Geomorphology*.;186:12-27.

Tang PFSA. (2012) Sensor Modeling of Laser Scanner for Automated Scan Planning on Construction Jobsites. *ASCE Libr*.:1-10.

Travelletti J, Delacourt C, Allemand P, et al. (2012) Correlation of multi-temporal ground-based optical images for landslide monitoring: Application, potential and limitations. *ISPRS J Photogramm Remote Sens*.;70:39-55.

Trier ØD, Pilø, Holger L. (2012) Automatic Detection of Pit Structures in Airborne Laser Scanning Data. *Archaeol Prospect*.;19(2):103-121.

Turner D, Lucieer A, de Jong S. (2015) Time Series Analysis of Landslide Dynamics Using an Unmanned Aerial Vehicle (UAV). *Remote Sens*.;7(2):1736-1757.

Wallace L, Lucieer A, Watson CS. (2014) Evaluating tree detection and segmentation routines on very high resolution UAV LiDAR ata. *IEEE Trans Geosci Remote Sens*.;52(12):7619-7628.

APPENDIX A. MODEL TIME CONTRIBUTION BREAKDOWN

*Man hours (not computer processing hours)
Y=Yes (model included that parameter)
N=No (model did not include that parameter)

Model Number: 1		
Model Parameters	Y/N	Time (hours)
Photo Selection*	Y	2
Est. Image Quality	Y	0.33
Masking*	N	-
Ground Control*	N	-
Camera GPS	N	-
Processing Quality	Med	-
Align Photos	Y	4.9
Dense Cloud	Y	5.74
	Total Time (hrs)	13.02
Number of Points:	8,770,924	Sparse
	67,492,215	Dense

Model Number: 2

Model Parameters	Y/N	Time (hours)
Photo Selection*	Y	2
Est. Image Quality	Y	0.33
Masking*	Y	2
Ground Control*	N	-
Camera GPS	N	-
Processing Quality	Med	-
Align Photos	Y	4.9
Dense Cloud	Y	5.65
	Total Time (hrs)	14.93

Number of Points:	7,770,245	Sparse
	56,202,493	Dense

Model Number: 3

Model Parameters	Y/N	Time (hours)
Photo Selection*	Y	2
Est. Image Quality	Y	0.33
Masking*	N	-
Ground Control*	Y	4
Camera GPS	N	-
Processing Quality	Med	-
Align Photos	Y	3.4
Dense Cloud	Y	15.33
	Total Time (hrs)	25.08

Number of Points:	8,770,989	Sparse
	66,647,794	Dense

Model Number: 4

Model Parameters	Y/N	Time (hours)
Photo Selection*	Y	2
Est. Image Quality	Y	0.33
Masking*	Y	2
Ground Control*	Y	4
Camera GPS	N	-
Processing Quality	Med	-
Align Photos	Y	3.0
Dense Cloud	Y	9.26
	Total Time (hrs)	20.57

Number of Points:	7,770,245	Sparse
	56,188,364	Dense

Model Number: 5

Model Parameters	Y/N	Time (hours)
Photo Selection*	Y	2
Est. Image Quality	Y	0.33
Masking*	N	-
Ground Control*	N	-
Camera GPS	Y	-
Processing Quality	Med	-
Align Photos	Y	3.6
Dense Cloud	Y	5.58
	Total Time (hrs)	11.51

Number of Points:	8,584,316	Sparse
	61,987,491	Dense

Model Number: 6

Model Parameters	Y/N	Time (hours)
Photo Selection*	Y	2
Est. Image Quality	Y	0.33
Masking*	Y	2
Ground Control*	N	-
Camera GPS	Y	-
Processing Quality	Med	-
Align Photos	Y	3.8
Dense Cloud	Y	5.62
	Total Time (hrs)	13.75

Number of Points:	8,619,288	Sparse
	55,963,381	Dense

Model Number: 7

Model Parameters	Y/N	Time (hours)
Photo Selection*	Y	2
Est. Image Quality	Y	0.33
Masking*	N	-
Ground Control*	Y	4
Camera GPS	Y	-
Processing Quality	Med	-
Align Photos	Y	2.5
Dense Cloud	Y	7.83
	Total Time (hrs)	16.65

Number of Points:	8,867,687	Sparse
	63,080,536	Dense

Model Number: 8

Model Parameters	Y/N	Time (hours)
Photo Selection*	Y	2
Est. Image Quality	Y	0.33
Masking*	Y	2
Ground Control*	Y	4
Camera GPS	Y	-
Processing Quality	Med	-
Align Photos	Y	3.1
Dense Cloud	Y	9.24
	Total Time (hrs)	20.66

Number of Points:	7,744,343	Sparse
	56,679,455	Dense

Model Number: 9

Model Parameters	Y/N	Time (hours)
Photo Selection*	Y	2
Est. Image Quality	Y	0.33
Masking*	N	-
Ground Control*	N	-
Camera GPS	N	-
Processing Quality	High	-
Align Photos	Y	4.9
Dense Cloud	Y	109.2
	Total Time (hrs)	116.4

Number of Points:	8,770,924	Sparse
	267,333,691	Dense

Model Number: 10

Model Parameters	Y/N	Time (hours)
Photo Selection*	Y	2
Est. Image Quality	Y	0.33
Masking*	Y	2
Ground Control*	N	-
Camera GPS	N	-
Processing Quality	High	-
Align Photos	Y	4.9
Dense Cloud	Y	30.04
	Total Time (hrs)	39.32

Number of Points:	7,770,245	Sparse
	221,506,960	Dense

Model Number: 11

Model Parameters	Y/N	Time (hours)
Photo Selection*	Y	2
Est. Image Quality	Y	0.33
Masking*	N	-
Ground Control*	Y	4
Camera GPS	N	-
Processing Quality	High	-
Align Photos	Y	3.4
Dense Cloud	Y	54.91
	Total Time (hrs)	64.64

Number of Points:	8,770,989	Sparse
	266,724,152	Dense

Model Number: 12

Model Parameters	Y/N	Time (hours)
Photo Selection*	Y	2
Est. Image Quality	Y	0.33
Masking*	Y	2
Ground Control*	Y	4
Camera GPS	N	-
Processing Quality	High	-
Align Photos	Y	3.0
Dense Cloud	Y	48.13
	Total Time (hrs)	59.45

Number of Points:	7,770,245	Sparse
	222,253,083	Dense

Model Number: 13

Model Parameters	Y/N	Time (hours)
Photo Selection*	Y	2
Est. Image Quality	Y	0.33
Masking*	N	-
Ground Control*	N	-
Camera GPS	Y	-
Processing Quality	High	-
Align Photos	Y	3.6
Dense Cloud	Y	31.51
	Total Time (hrs)	37.45

Number of Points:	8,584,316	Sparse
	246,009,525	Dense

Model Number: 14

Model Parameters	Y/N	Time (hours)
Photo Selection*	Y	2
Est. Image Quality	Y	0.33
Masking*	Y	2
Ground Control*	N	-
Camera GPS	Y	-
Processing Quality	High	-
Align Photos	Y	3.8
Dense Cloud	Y	37.87
	Total Time (hrs)	46.01

Number of Points:	8,619,288	Sparse
	222,284,354	Dense

Model Number: 15

Model Parameters	Y/N	Time (hours)
Photo Selection*	Y	2
Est. Image Quality	Y	0.33
Masking*	N	-
Ground Control*	Y	4
Camera GPS	Y	-
Processing Quality	High	-
Align Photos	Y	2.5
Dense Cloud	Y	43.32
	Total Time (hrs)	52.16

Number of Points:	8,867,687	Sparse
	252,257,488	Dense

Model Number: 16

Model Parameters	Y/N	Time (hours)
Photo Selection*	Y	2
Est. Image Quality	Y	0.33
Masking*	Y	2
Ground Control*	Y	4
Camera GPS	Y	-
Processing Quality	High	-
Align Photos	Y	3.1
Dense Cloud	Y	70.04
	Total Time (hrs)	81.46

Number of Points:	7,744,343	Sparse
	223,226,048	Dense

APPENDIX B. MODEL ACCURACIES

All accuracies listed in centimeters

Model #	Trial 1	Trial 2	Trial 3	Trial 4	Trial 5
1	1.01	1.25	1.11	3.43	1.74
2	1.07	1.17	1.49	4.17	1.57
3	0.94	1.29	1.03	1.02	1.62
4	1.22	1.01	1.38	1.01	1.52
5	1.20	1.52	2.42	1.30	2.00
6	1.13	1.36	1.44	2.28	2.19
7	1.03	1.39	6.21	1.55	1.39
8	1.29	1.01	1.65	1.60	1.41
9	1.03	1.07	1.02	1.28	1.30
10	1.07	1.02	1.04	1.07	0.91
11	0.91	0.81	0.86	0.91	1.37
12	1.53	1.40	1.24	1.10	0.95
13	1.07	0.98	0.89	1.65	1.17
14	1.03	1.81	1.57	1.15	1.01
15	0.95	0.83	1.13	1.11	1.51
16	0.95	1.05	0.98	1.00	1.14

Model #	Trial 6	Trial 7	Trial 8	Trial 9	Trial 10	Average
1	1.81	1.91	1.58	1.76	2.23	1.78
2	1.81	1.37	1.71	1.06	1.71	1.71
3	1.35	1.28	1.48	2.15	1.43	1.36
4	1.28	1.12	1.19	1.46	1.84	1.30
5	1.48	1.72	3.00	1.66	1.72	1.80
6	2.11	1.54	1.70	3.21	1.49	1.85
7	2.12	1.33	1.07	0.97	1.50	1.86
8	1.59	1.48	1.00	1.37	1.73	1.41
9	1.95	1.45	1.47	1.80	1.46	1.38
10	3.47	1.32	1.16	1.20	1.41	1.37
11	0.94	1.80	1.18	1.50	1.24	1.15
12	1.19	1.00	1.57	0.96	1.13	1.21
13	1.21	2.72	1.09	1.30	1.45	1.35
14	1.33	1.86	0.85	1.44	0.97	1.30
15	1.55	1.00	1.01	1.19	1.21	1.15
16	1.19	1.79	1.53	1.83	1.48	1.29